

**MAX-PLANCK-INSTITUT FÜR PLASMAPHYSIK
GARCHING BEI MÜNCHEN**

**A Data Bank of Disruptive Discharges
in ASDEX**

Ch. Ludescher*, J. Gernhardt, K. Lackner,
F. Schneider, ASDEX Team

IPP 5/48

March 1994

* Princeton Plasma Physics Laboratory, Princeton, N.J. 08540, USA

*Die nachstehende Arbeit wurde im Rahmen des Vertrages zwischen dem
Max-Planck-Institut für Plasmaphysik und der Europäischen Atomgemeinschaft über
die Zusammenarbeit auf dem Gebiete der Plasmaphysik durchgeführt.*

Abstract

The compilation of data banks relating to plasma disruptions is important for the design of next-step devices and tokamak reactors, as a means of establishing safe operation regimes and assessing the residual risk from such events. ASDEX has an operational history of 33509 plasma shots covering an exceptionally wide range of machine conditions: Divertor/limiter configurations; Ohmic, NBI, ICRH and LH heating; carbonization, boronization wall-conditioning, gas-puff and pellet refuelling. We have compiled a data base of the Disruptive Operational Regimes in ASDEX (DORA), which contains the relevant information for all ASDEX-discharges and is available on tape and readable by different data bank systems for further evaluation. In the present report we first describe the criteria applied to recognize and classify disruptions and the information about them stored in the file. In a second part we use the the DORA file for some sample applications of physical or engineering interest. In an appendix we give the data and format information necessary to read the DORA file.

A DATA BANK OF DISRUPTIVE DISCHARGES IN ASDEX

Ch. Ludescher*, J. Gernhardt, K. Lackner, F. Schneider, ASDEX Team

Max-Planck-Institut für Plasmaphysik, EURATOM Association
D-8046 Garching

*Princeton Plasma Physics Laboratory, Princeton, N.J. 08540, USA

1. INTRODUCTION

The compilation of data banks relating to plasma disruptions is important for the design of next-step devices and tokamak reactors as a means of establishing safe operation regimes and assessing the residual risk from such events. At the same time, the use of such data banks in statistical analyses or as a catalogue for selecting cases for in-depth studies should help to advance our physical understanding of the preconditions and dynamics of the disruptive instability.

ASDEX has an operational history of 33509 plasma shots covering an exceptionally wide range of machine conditions:

Divertor/limiter configurations: ASDEX used single-null and double-null divertor configurations with two different divertor chamber geometries (differing also in the target plate material: Ti and Cu, respectively) and several different arrangements of bypasses between the divertor and the main plasma chamber. A limited number of discharges were carried out with mushroom or poloidal limiters, and two campaigns used continuous toroidal limiters made of steel and graphite, respectively.

Machine parameters: ASDEX varied the plasma current in the range $90 \text{ kA} < I_p < 500 \text{ kA}$, the main field between $-0.5 < B_t < 5.9 \text{ T}$, and the plasma density (during current plateau conditions) between $1.0 \times 10^{18} \text{ m}^{-3} < \bar{n}_e < 1.5 \times 10^{20} \text{ m}^{-3}$, where the lower extreme of the density values corresponds to slide-away and the higher extreme to pellet-refuelled discharges. The cylindrical safety factor at the boundary q_{cyl} reached extreme values of >14.5 and <1.9 , respectively, during current plateau conditions.

Additional heating methods: ASDEX used three heating systems at power levels in the multi-MW range: NBI (D^0 , H^0), ICRH in the 2nd-harmonic and minority

heating regimes, and LH with symmetric and current drive spectra at 1.3 and 2.45 GHz. During a limited campaign, Alfvén wave heating was also used.

Wall-conditioning techniques: ASDEX used, at different times, carbonization and boronization in the main discharge chamber and Ti-gettering in the divertor.

Refuelling: ASDEX applied gas-puffing in the main and divertor chambers, and used single-pellet and multi-pellet injectors with pellets of different magnitude and velocity.

These different operating conditions also allowed access to a number of different plasma regimes, some of which were first recognized on ASDEX, and which are of great relevance to the performance of next-step devices. The operations also extensively explored the beta limit in circular discharges and the density limit under different heating and refuelling scenarios.

To make the information on disruptions that was gained over this wide operating range amenable to systematic and statistical evaluation by the team and the scientific community, we designed a data base, called DORA (Disruptive Operational Regimes in ASDEX), and have started to fill it with the corresponding discharge data. The data are in the format of a VAX data file, available on tape and readable by different data bank systems for further evaluation.

As an inherent conflict exists between the two goals: (1) to cover all discharges, including the relatively early ones, and (2) to give also information utilizing the latest diagnostic developments, we designed the DORA data file to the diagnostic status of the last discharge campaign, but set flags to indicate the possible non-availability of a particular signal. This will allow us to utilize the full ASDEX experience in more cursory analyses of operational aspects (i.e. mapping out of the regimes leading to disruptions and characterization of the severity of the machine stresses resulting from the different disruptions under different discharge conditions) and to use subsets, from more recent experimental campaigns only, for more in-depth, physical investigations. Some discharge data envisaged in DORA were not available for all shots in an immediately machine-readable form: these will eventually be filled in by extracting them manually from the log-books.

In the present report we describe the criteria applied to recognize and classify disruptions and the information about them stored in the file. These quantitative criteria, as well as the

timing of taking the stored data, required decisions which in some cases clearly involve an element of arbitrariness. We try to give for each case the rationale for our particular choice (which was often based on the time resolution and noise level of particular diagnostic signals). In several cases we believe, however, that the precise choice is less important than a clear definition and consistent, uniform application of the particular criterion.

In a second part of this report, we use the DORA file in its present form, covering the last 22,000 shots prior to the final shut-down, for some sample applications of physical or engineering interest.

In an appendix we give the data and format information necessary to read the DORA file.

2. CONTENTS OF THE DORA DATA BANK

For this data bank, a disruption is defined as a sudden loss or expulsion of magnetic or thermal energy from the plasma column. This definition also includes the sudden β -drops sometimes observed during β -limit studies, which may have no significant effect on the plasma current and might plausibly have a quite different origin from conventional disruptive instabilities. We intentionally kept this definition rather broad, leaving it to the user of the data bank to discriminate between different types of event on the basis of the additional stored information. As several such events may occur in one discharge, we restrict ourselves to the first one (labelled first) and the one ultimately ending in the current I_p going to zero (labelled terminal disruption). We also excluded the very early discharge phases from our examinations, completely omitting from our data base shots not reaching 20 kA or not lasting longer than 50 ms completely.

All other shots - either suffering disruptions or coming to a peaceful end - are included in the data bank. The purpose of including the latter (characterized by certain peak or plateau parameter values) is obviously to allow positive mapping of safe regimes of operation as well.

2.1 Quantitative Criteria for Recognizing a Disruption

The programme used for automatic recognition will identify a disruption if at least one of the following criteria is satisfied:

a) I_p has a positive hump with an amplitude $\delta I_p/I_p \geq 0.02$. To identify the hump, we require that I_p increases from a given value I_{p0} to a value $\geq 1.02 \times I_{p0}$ and returns to $\leq 1.0 \times I_{p0}$ within 20 ms. (This criterion recognizes the positive current spike corresponding to the poloidal flux expulsion and the sudden decrease of the internal inductivity l_i . For our diagnostic system, this is a more reliable signal than the accompanying negative voltage spike.)

b) The difference between B_{pol} measured on the larger and smaller major radius sides of the plasma column decreases by

$$|\delta (B_{pa} - B_{pi}) / ((B_{pa} + B_{pi})/2)| = |\delta X| > 0.07 (\Lambda + 1)$$

within 5 ms, where $\Lambda+1$ is the Shafranov parameter computed in the same program. (This criterion should detect a sudden loss of thermal plasma energy; the trigger criterion is chosen so as not to react to the β -decay following a sudden switch-off of the power, if the energy confinement time is 25 ms or longer.)

c) The plasma current decays within 100 ms from a plateau to less than 50 kA. To avoid recording as "first" disruption magnetic perturbations occurring during the current-build-up phase, we neglect disruptions after which the current increases by a further 25% .This criterion therefore nevertheless allows recording of terminal disruptions in the build-up phase.

Terminal disruption is defined as the first one after which the current decays within the next 25 ms by more than 16%. In our later operation phases, our current control system has included an algorithm for a real-time recognition of disruptions. The system was programmed to ramp down the plasma current within 200 ms after each recognized disruption. We therefore label as terminal only disruptions for which the initial current decay rate exceeds this intended one by more than 50%. The time till $I_p = 50$ kA is recorded, however, also for the non-terminal disruptions included. (This latter limit is uniformly used by us for defining the end of the discharge.)

Figure 1 shows a sample set of disruptive discharges with quite different characteristics which were used in the development phase of our automatic recognition code for debugging. For each of the eight cases, the current (I_p) and line-averaged density (\bar{n}_e) curves are shown over a time span of 3 s. The vertical lines indicate the recorded

disruption times, with the letters F and T indicating, when applicable, the first and the terminal disruption.

2.2 Data Stored for Each Recorded Discharge

As mentioned before, we generate an entry for each discharge with a duration longer than 50 ms reaching a plasma current larger than 20 kA. For each discharge we record the information described in Sects. 2.2.1 and 2.2.2 (all quantities are expressed in SI -units).

2.2.1 General machine preconditions

Information on the following items describing the general machine conditions and the principal investigative aim of each discharge (in the form of key numbers) is available for the more recent ASDEX shots in computer-readable form. For these cases the information has also been read into the present data bank. For earlier discharges it is planned to extract and include the equivalent information manually from logs at a later stage:

Starting with shot number 25979:

- shot number since last machine opening,
- shot number since start of daily operation,
- shot number since last discharge cleaning,
- shot number since last wall treatment with
 - argon,
 - boron,
 - carbon,
 - deuterium,
 - helium,
 - titanium.

Starting with shot number 25777:

- divertor configuration (double null or single null, top or bottom),
- type of experiment,
- MAC log theme (a key number associated with a text file describing the investigative aim),
- known machine faults such as a leak, a probe in protruding position, impurity injection experiment (has to be read in from logs: a 16-character field is provided in the data file).

2.2.2 Discharge history up to disruptive or peaceful discharge end

For each discharge included in the data bank, we record:

- the total discharge duration (from the time I_p exceeds 20 kA till it drops below 50 kA),
- the time of beginning of current plateau, defined by the satisfaction of both
 - a) $\delta I_p < 5\%$ of I_p over 100 ms and
 - b) $I_p > 95\%$ of max (I_p), where a possible current peak at the disruption is disregarded in the definition of the maximum of the current. (the second criterion is of importance for cases in which several current plateaus were generated in the course of one discharge)
- the time of the end of the current plateau, defined by the reverse criteria as the beginning
- the time of the end of the discharge (current drops below 50 kA).
- B_ϕ , the toroidal field strength at the nominal radius $R_0 = 1.65$ m

Furthermore we record the extremal values and the times, when they occur, of the following parameters, selected - unless otherwise noted - over the time interval starting with the instant at which I_p reaches 20 kA and ending 50 ms before either the first disruption or the end of the discharge. For non-disrupting discharges, these parameter values are used to identify potentially stable regimes of operation. They are used, for example, in sect. 3 to establish the Hugill diagram for non-disruptive discharges:

n_e	maximum value of line-average density,
I_{p-ne}	plasma current at time of n_e ,
I_p	maximum value of plasma current,
q_{cyl}	minimum value of cylindrical, circular q at the boundary, based on $a = 0.4$ m, $R_0 = 1.65$ m,
$d n_e / dt$	maximum value averaged over 20 ms,
$d I_p / dt$	maximum value averaged over 20 ms,
$\beta_{pol+l_i/2}$	maximum value and value at middle of plateau,
U_{loop}	loop voltage projected to the plasma surface, minimum value and value at middle of plateau,
P_{rad}	total power radiated from the plasma in the main chamber (bolometrically measured) at middle of plateau,
Z_{eff}	at middle of plateau (based on spatial constancy of E-field and Z_{eff} , T_e -profiles from YAG-Thomson scattering and Spitzer conductivity)
l_i	at middle of plateau (based on same prescription as Z_{eff})

- $\int P_{OH}(t) dt$ OH energy deposited in the plasma up to 50 ms before disruption or discharge end,
 $\int P_{ICRH}(t) dt$ total deposited ICRH energy,
 $\int P_{LH}(t) dt$ total deposited LH energy ,
 $\int P_{NI}(t) dt$ total deposited NI energy,
 - sawteeth: did they occur (1) at any time, (2) before end of current build-up phase (an automatic recognition procedure is used which takes as input the HCN line-integrated density. It recognizes only sawteeth which have
 - (a) time period < 30ms , and
 - (b) consist of a train of more than 5 sequential teeth of same (± 1 ms) period)
 - pellets: at any time during discharge,
 - gas: main plasma constituent,
 - lock: time of start and end of lock (starting with shot 30759)
 - add. heating: time of start and end of heating pulse and maximum input power and
 total energy for NBI, ICRH, LH. (Times for LH are from (channel 30, LH); max power input from MAC EXCEL database; energy for LH is not available)

2.2.3 Plasma conditions immediately before disruption(s)

All values are stored for the first and terminal disruptions. (If the first disruption is also terminal, it is labelled terminal in our file.) These data are assumed to identify the immediate preconditions for a disruption. In Sect. 3 of the present report they are used, for example, to draw the Hugill diagram for disrupting discharges:

- I_p average taken over last 50-10 ms before disruption,
 n_e average taken over last 50-10 ms before disruption,
 $\langle d I_p / dt \rangle$ average taken over last 50-10 ms before disruption,
 $\langle d n_e / dt \rangle$ average taken over last 50-10 ms before disruption.

The following values are taken 20 ms before disruption(s)(the timing being determined by the fact that the YAG-laser system fires every 16 ms and the necessity to ensure that the interpolated values taken for some of the analyses are not contaminated by values taken during or after the disruption):

- R
 z

$\beta_{pol+l_i/2}$
 U_{loop}
 q_{cyl}
 P_{rad}
 l_i computed as above,
 Z_{eff} (see l_i).

2.2.4. Parameters describing the plasma dynamics of the disruptive instability

The following values are stored for the first and terminal disruptions:

- MHD precursor characterization: a signal (channel 33, MHDA), measuring dB_{θ}/dt in the outside mid-plane is recorded. (the particular signal being chosen because it has been generally available with adequate time resolution for quite some time)

(a) if the disruption is recognized via a current spike: in the form of its maximum over 20 ms prior to start of spike,

(b) if the disruption is recognized by one of the other two criteria: in the form of its maximum amplitude between 25 to 5 ms prior to disruption.

(This signal records of course not only mode activity, but also the axisymmetric perturbations accompanying the disruption and the follow-up phase. For this reason we exclude in case (b) - where the identification of the disruption has a possible jitter of 5 ms due to the low sampling rate - the last phase from our record.)

If the first and terminal disruption are less than 20ms apart, the value for the second (terminal) disruption is stored as a negative number (to alert us to the possibility that the signal might be more characteristic of the - possibly axisymmetric - post-cursor behaviour of the first rather than the pre-cursor behaviour of the terminal disruption).

- the total expelled flux during the negative voltage spike

$$\mu_0 R (\ln(8R/a) - 2) * (I_{p,max} - I_{p,o}),$$

where $I_{p,o}$ and $I_{p,max}$ are the plasma currents immediately before and at the height of the disruption spike, respectively. (This value can be related to the change of l_i during the disruption and to the total poloidal field energy ejected through the plasma surface under the assumptions of either poloidal flux conservation between the magnetic and torus axis, or of negligible magnetic energy dissipation during this phase. It should thus be a good measure of the intensity of the disruptive event.)

The following values are based on terminal disruption only; they are supposed to be relevant for the stresses experienced by the PF-circuitry and the vessel:

- number of further disruptions before I_p falls below 50 kA (Frequently the current decay following a disruptive event recognized by our program as terminal proceeds in a sequence of cascades, separated by further disruptive events. The latter are recognized by the same criteria as given in 2.1.1.);

- $(-d \ln I_p / dt)$: maximum value of the current decay rate from the instant of the terminal disruption till our recorded discharge end ($I_p = 50$ kA);

- displacement of plasma current channel during the disruptive current decay

$$\int (R(t) - R_{20}) I_p(t) dt / \int I_p(t) dt \quad (\text{channel 31, DHOR})$$

and

$$\int (z(t) - z_{20}) I_p(t) dt / \int I_p(t) dt \quad (\text{channel 31, DVER})$$

from terminal disruption till end ($I_p = 50$ kA). The reference radius R_{20} and the vertical plasma position z_{20} are taken at 20 ms prior to the disruption. (The weighting of the plasma displacement by the instantaneous current is done to give a better overview of the resulting forces on external structures.);

- maximum displacement of plasma current channel during discharge

$$\max |(R(t) - R_{20}) I_p(t)|$$

$$\max |(z(t) - z_{20}) I_p(t)|$$

- hard X-rays, as recorded by channel 22, signal R1:

- a) maximum count taken at terminal disruption ± 3 ms

- b) maximum count taken over 100 ms prior to the terminal disruption and time instant to which it refers

(The hard X-ray emission following the disruption is presumably a sign of the loss of confinement of the runaway electrons. As the total amount of runaways present in the machine prior to this moment is, however, a complicated function of the whole discharge history, we also provide the reference signal (b).).

2.2.5 Short characterization of the disruption behaviour of the discharge

This information is partly extracted from the other data recorded and is also supposed to serve for fast selection of shot subsets for statistical analyses:

- time of first and terminal disruptions,
- criteria how disruption is recognized by program,
- condition terminal disruption occurred during:
 - current buildup,
 - current plateau
 - current decay,
 - density increase,
 - neutral injection,
 - lower hybrid heating,
 - ion cyclotron heating,

2.2.6. Information on the existence and validity of the data in the file

- Status of validity/existence of channels read
 - time, when density, channel (44,H1), becomes invalid (time = 0 indicates signal is $> 4 \times 10^{18}$ at end of discharge). Criterion for the validity is an increase by more than 4×10^{18} between sampling.
- Status of validity of temperature profile (YAG)
- Status of origin of information
 - MYKENN (Pellet, gas, divertor configuration, additional heat - for pellet shots > 14000)
 - MAC log (Wall-Conditioning divertor configuration and aim of experiment - since shot 25777)
 - H-MODE List (max NI power, gas - for all H-Mode shots - channel (5,PNI) is not valid before shot 25776)
 - LH MAC database (max LH power and phase - for shots > 26434)

3. DISRUPTION BEHAVIOUR OF ASDEX IN THE "HARDENED" DIVERTOR GEOMETRY

For the compilation of the DORA data bank we examined all of the 33509 ASDEX discharges, of which 26991 satisfy the criteria for inclusion; i.e. they lasted longer than 50 ms and exceeded a plasma current of 20 kA (some shots are missing because they could not be read from the optical media). As sample application we give here some results on the disruption behavior of ASDEX during the operational phase from April 87 to August 89, corresponding to shots #20 283 to 29 296, making simple use of the DORA data bank without application of statistical code packages. This phase corresponded to a period immediately after "hardening" of the ASDEX divertor structure, to make it compatible with steady state heat loading. This discharge campaign was also distinguished by the attempt to push all heating systems to higher pulse lengths, and - since December 88 - by extensive operation of a 2.45 GHz lower hybrid system in current-drive and electron-heating mode. During this phase each of our three available additional heating systems (NBI, LH, ICRH) reached powers launched into the vessel in excess of 2 MW. Of the discharges considered here, 33% of them are totally disruption-free (according to our definitions in section 2.2) whereas 37% suffer a disruption during the current plateau.

3.1 Severity of Disruptions

Our data base contains two parameters which constitute simple measures of the severity of a disruptive discharge:

- (1) the expelled flux $\Delta\Phi_d$, which is exclusively determined by the internal plasma dynamics (the magnitude of the accumulated unstable potential),
- (2) the current decay rate, which is probably also sensitive to - in addition to the above facts - the form of plasma-wall interaction taking place during the rapid phase and the degree of external discharge control still possible after the MHD-event.

Figures 2a and 2b show histograms of the number of non-terminal and terminal disruptions as a function of the expelled flux. The capability of the plasma to survive a disruption without subsequent rapid current decay is clearly linked to the magnitude of the expelled flux. So, 65% of all discharges survive a disruption with a flux expulsion of less than 0.01 Vs, but only 12% one larger than 0.04 Vs. Terminal disruptions can result from events with very small flux loss, but have a broad maximum in their distribution around $\Delta\Phi_d = 0.13$ Vs. This maximum becomes more pronounced if the expelled flux is normalized by the plasma current (Fig. 2c). Converted formally to an equivalent internal

inductivity change by $\Delta l_i = 2 \Delta \Phi_d / (\mu_0 R I_p)$, this peak in the distribution is located around $\Delta l_i \approx -0.35$.

The plasma current decay rate following the fast, non-axisymmetric phase of the disruption is another measure of the intensity of an event. Of relevance are both the maximum rate of decay - which is usually assumed right after the transient overshoot of the plasma current - and the average rate, defined in the following by

$$\left\langle \frac{d I_p}{I_p dt} \right\rangle_{\text{dec}} = \frac{2 (I_{p0} - 50 \text{ kA})}{(I_{p0} + 50 \text{ kA}) \cdot (t_{\text{end}} - t_{\text{disrupt}})}$$

Histograms for both measures show clear statistical distributions with maxima at decay time constants of 13 and 60 ms for, respectively, the phase of fastest decay (Fig. 3a) and the time averaged rate (Fig. 3b). Both distributions have, however, a long tail, and 357 discharges (4.2%) have a faster peak rate than 200 s^{-1} (corresponding to a 5 ms decay time) and 204 (2.5%) a higher average rate than 100 s^{-1} . More than half of these disruptions (118) with an average current decay rate $>100 \text{ s}^{-1}$ start out from the current plateau. Exceptionally hard disruptions, identified by a search of the DORA data bank, should probably be investigated in individual case studies to associate them with particular machine conditions. So, the hardest disruption out of a current plateau recorded among the last 8 389 shots (#28 396), with an average current decay rate of 536 s^{-1} , resulted from an unintended partial shunt of the divertor coils, and hence a limiter discharge with an uncontrolled contact surface. The five runners-up among the last 2 000 shots (#28467, #27883, #28195, #28166, #28883) with average decay rates from the plateau between 105 s^{-1} and 395 s^{-1} , were all cases with high lower hybrid power and low plasma density, and fall into a narrow window around $q_{\text{cyl}} \approx 3.3$.

The sudden loss of thermal and poloidal field energy from the plasma corresponds to a reduction in the outward directed hoop force and thus leads to an inward shift of the plasma column which is limited only by induced vessel currents and - on a longer time scale - by the action of the feedback system. The magnitude of the radial displacement during the post-disruptive current decay is thus also a measure of the disruption severity. Figure 4a also shows for this parameter the statistical distribution, which has a well-defined maximum at around -3.5 cm.

ASDEX was designed with an average field decay index of the applied poloidal fields $n = -d \log B_{\text{vert}} / d \log R \approx 0.5$. The plasma column is thus inherently stable against displacements, and not subject to so-called "vertical" disruptions. It does, however, have passively conducting structures above and below the main plasma, and for vertically displaced discharges the reduction of the plasma current will cause an attractive force towards the nearer structure. The resulting displacement is limited, however, by the

stabilizing curvature of the vertical field. In fact, a plot of the average (current-weighted) vertical displacements of the plasma column during the post-disruption phase (Fig. 4b) shows a predominant tendency of the discharge to remain well-centred. Some of the discharges, however, are slightly - by less than a centimetre - displaced in the vertical direction, with a preference for the upward direction in line with the tendency to run single-null discharges on ASDEX predominantly linked to the top divertor chamber.

The expelled flux, the rate of current decay, and the inward displacement of the plasma column are all measures of the severity of a disruptive event, and one would thus expect a strong correlation between these parameters. In fact, there is a tendency, at least with the bulk of the data, for the radial displacement (Fig. 5a) and the peak current decay rate (Fig. 5b) to increase with the amount of flux expelled.

3.2 Stable and Disruptive Operational Regimes

We have chosen two common representations of discharge parameters to look for evident correlations with the occurrence of disruptive instabilities. One is a histogram of disrupting and non-disrupting shots as a function of q_a (Fig. 6), where the safety-factor values refer to the current plateau, and disruptions are only included when occurring during this phase. As no further selection criterion was applied to these data, the danger of misinterpreting a possible operational bias (such as a particularly aggressive heating campaign at a given B_t , I_p - combination) as a physical effect linked to a particular value of q_a is of course high. One is nevertheless tempted to recognize in these data the existence of some q_a -regions of particular resilience or particular sensitivity, which should be further investigated in more detail.

Figures 7a-c show the location of non-disrupting and disrupting discharges in the Hugill diagram $n_e R / B_t$ vs. q_a .

Acknowledgements:

The authors are indebted to Dr. H. Zohm for fruitful discussions.

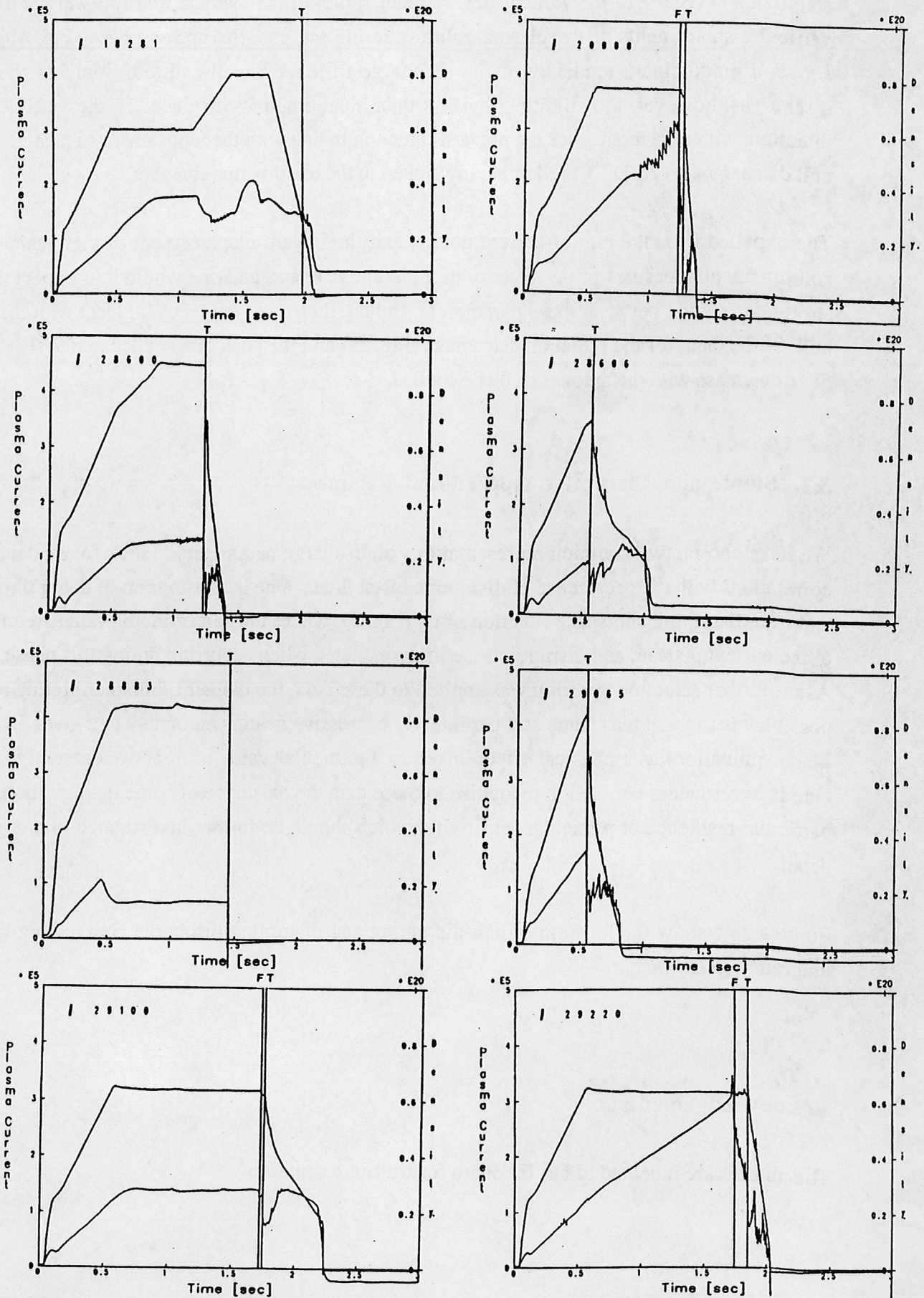


Fig. 1: Time traces for I_p and \bar{n}_e for disruptive ASDEX discharges taken as test-cases for the automatic disruption recognition procedure. Vertical lines indicate time-instances of recognized first (F) or terminal (T) disruptions.

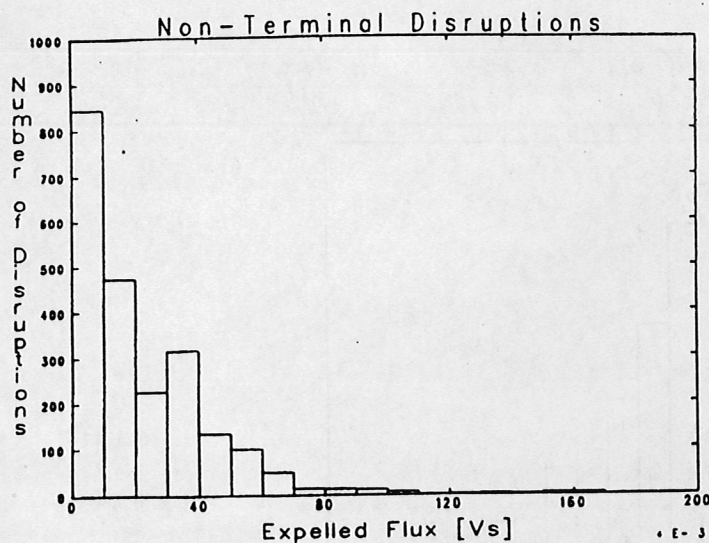


Fig.2a: Histogram for the flux expelled during the negative voltage spike phase of non-terminal disruptions.

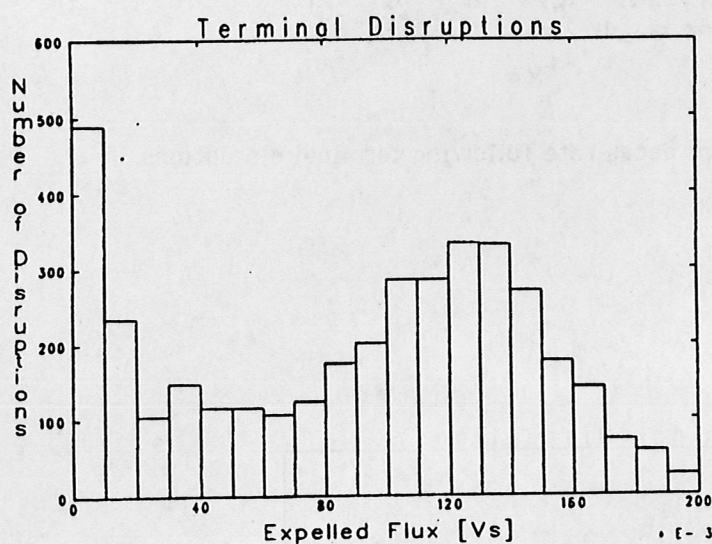


Fig.2b: Histogram for the flux expelled during the negative voltage spike phase of terminal disruptions.

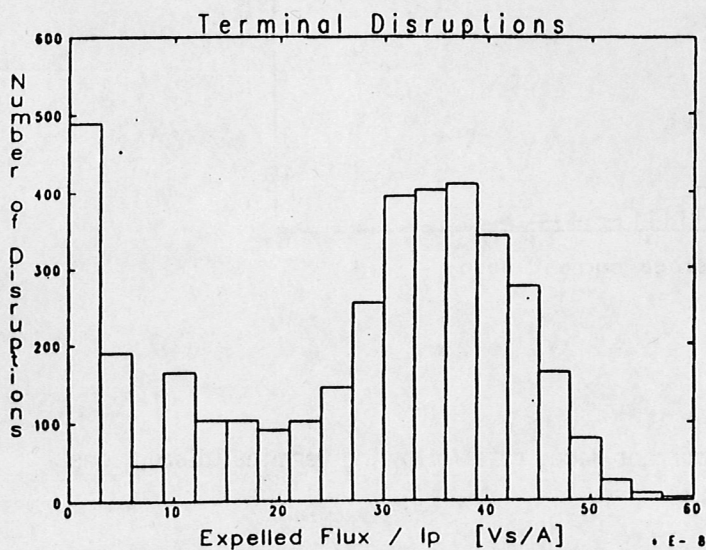


Fig.2c: Histogram for the expelled flux, normalized to the plasma current, for terminal disruptions.

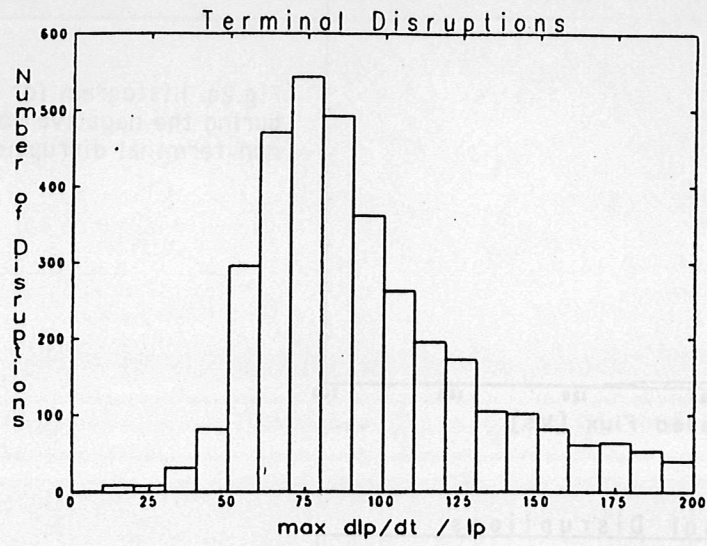


Fig.3a: Histogram for the maximum current decay rate following terminal disruptions.

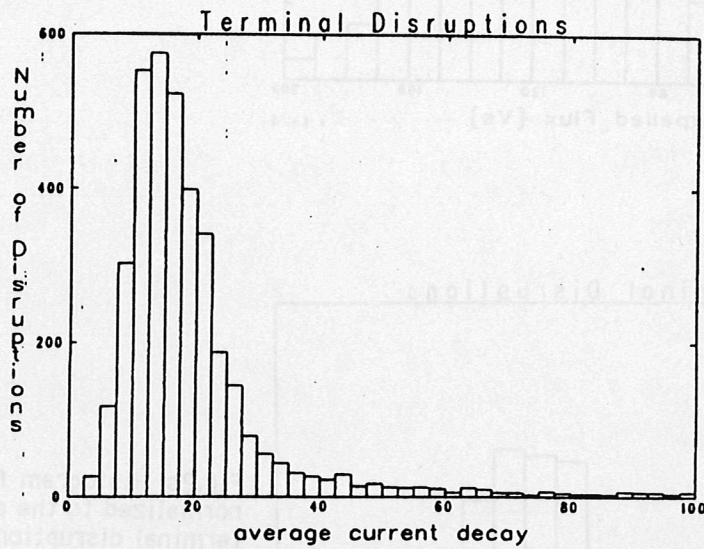


Fig.3b: Histogram for the time-averaged current decay rate following terminal disruptions.

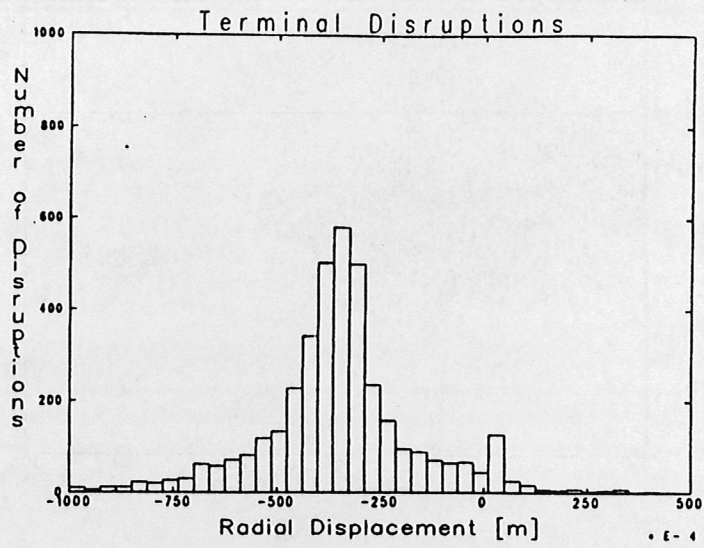


Fig.4a: Histograms for the radial plasma displacement during terminal disruptions.

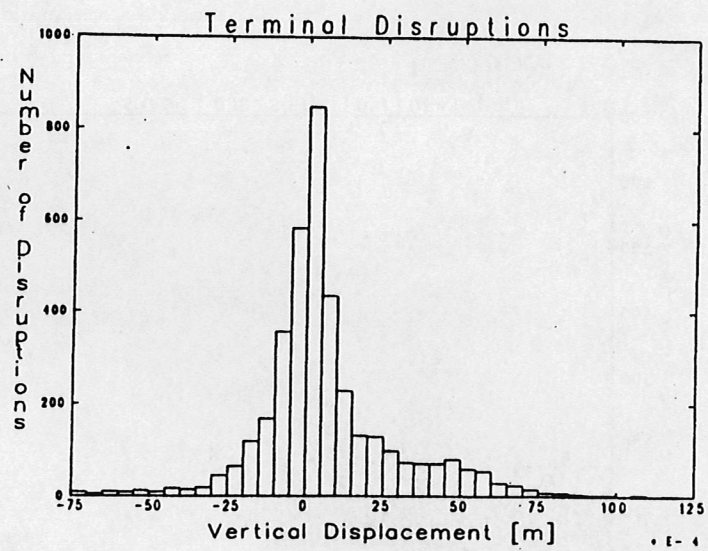


Fig.4b: Histograms for the vertical plasma displacement during terminal disruptions.

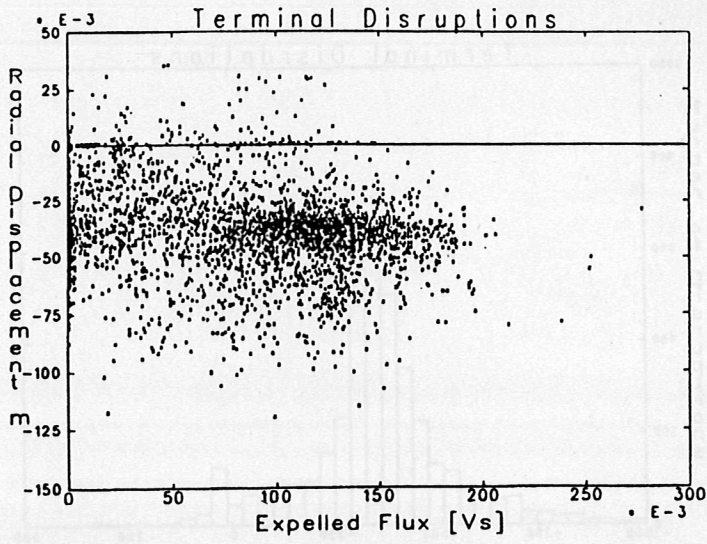


Fig.5a: Relation between the radial displacement of the plasma column and the expelled flux during terminal disruptions.

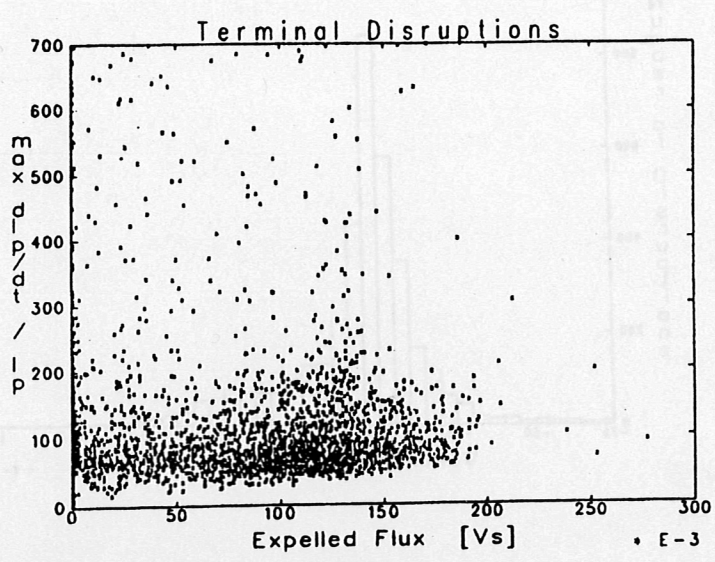


Fig.5b: Relation between the maximum current decay rate and the expelled flux during terminal disruptions.

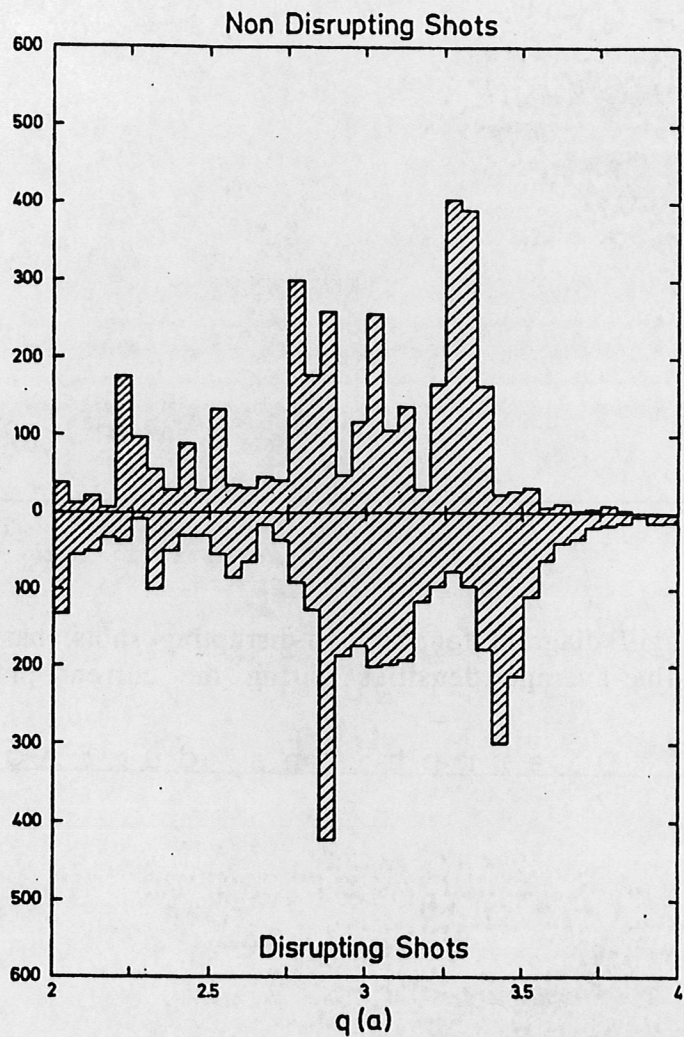


Fig.6: Histogram of non-disruptive (upper part) and disruptive (lower part) discharges as a function of q_a . Data refer to the current plateau phase, and only disruptions during this phase are included.

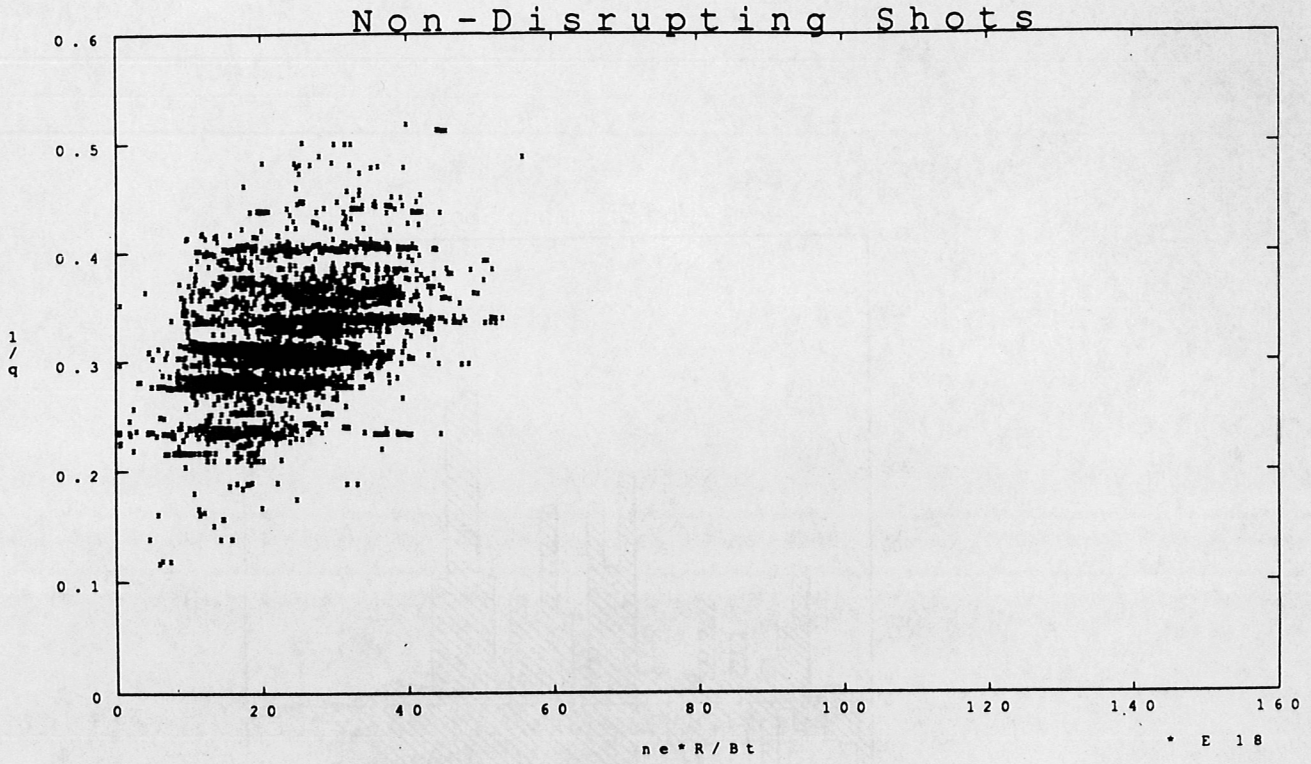


Fig. 7a: Hugill diagram for the non-disrupting shots, based on the maximum line-average densities during the current plateau.

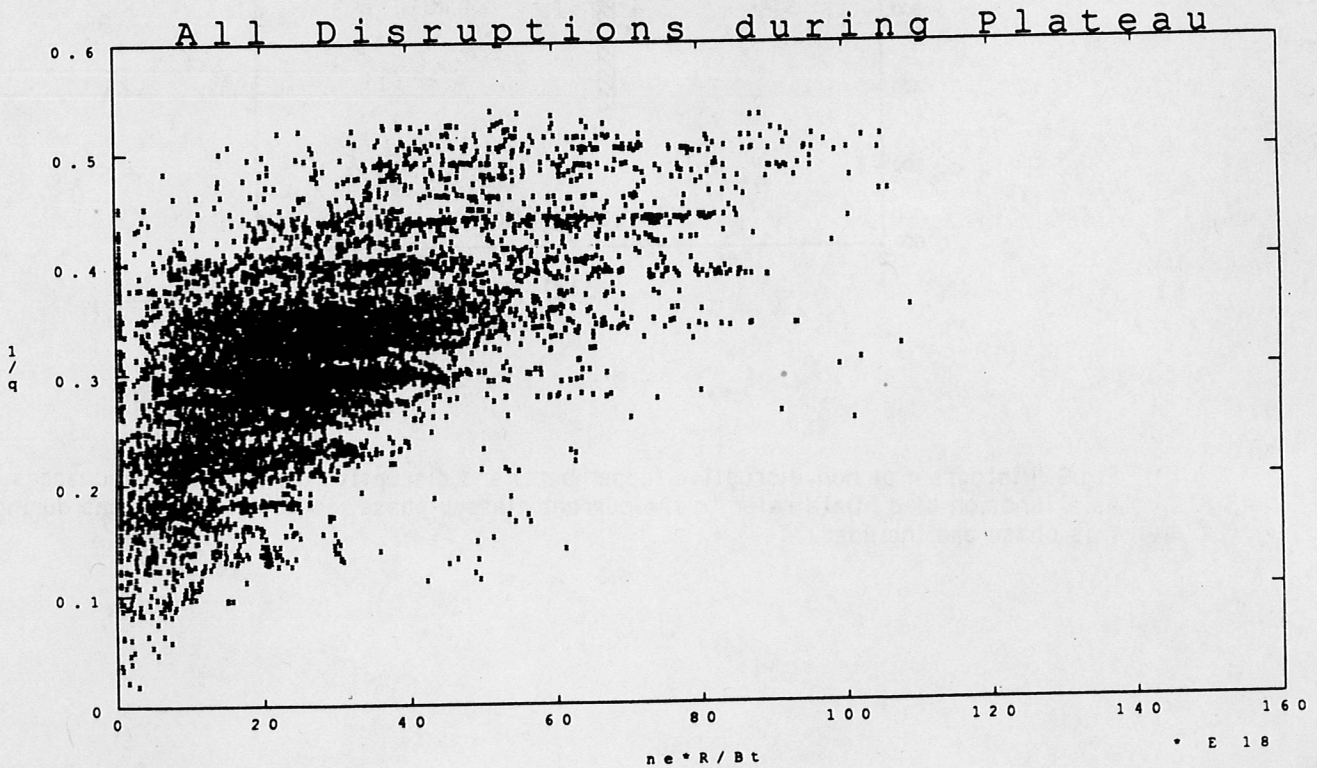


Fig. 7b: Location of plasma parameters in the Hugill diagram, prior to terminal disruptions during current plateau phase.

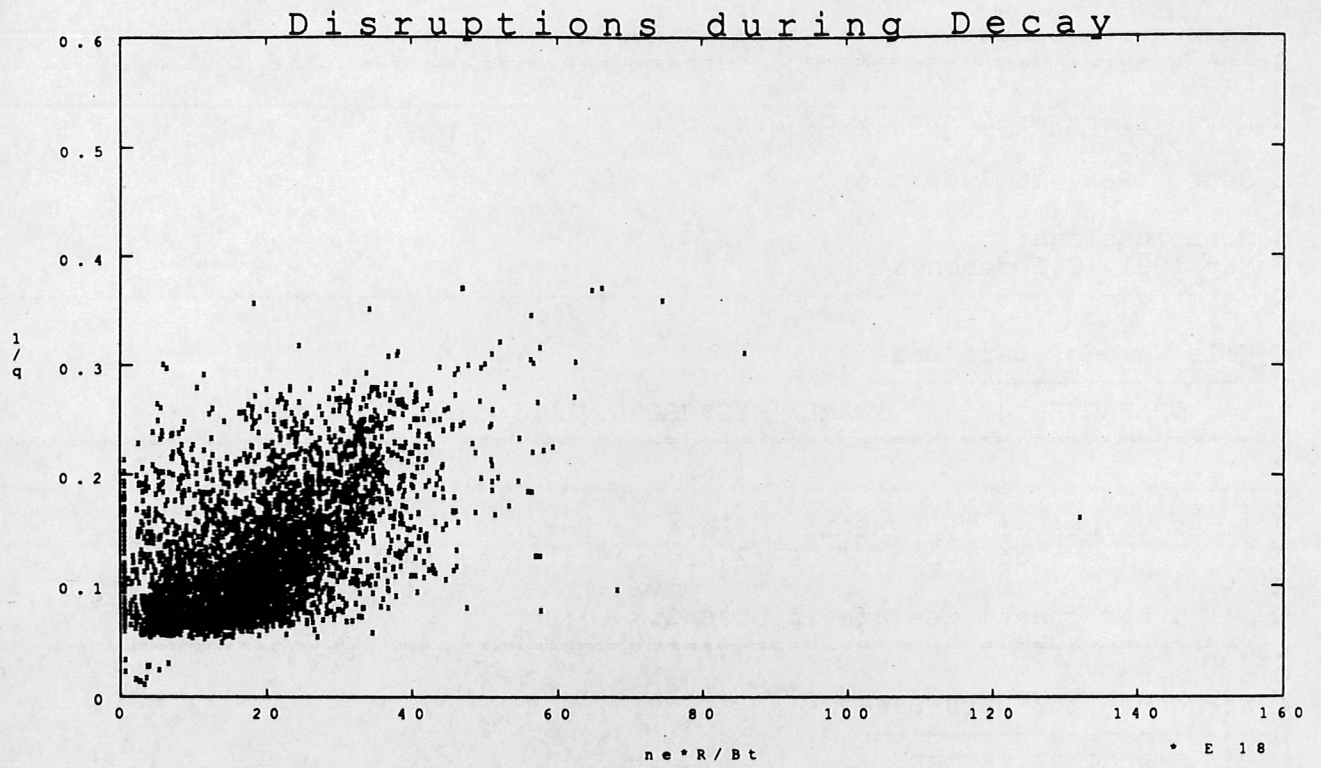


Fig. 7c: Location of plasma parameters in the Hugill diagram, prior to disruptions during current ramp-down phase.

APPENDIX: DORA file information

```

C
C Disruptive Operational Regimes in ASDEX ( D O R A )
C=====
C
C Definitions of Contents of Data base
C
C Sept. 1989, C.Ludescher
C
C Modifications:
C May 1991, C.Ludescher
C-----
C
C File Name of Data Base
C-----
C CHARACTER*40 FNAME/'SYS$USERA:[LUDESCHER.DATA]DORA.DAT'/
C=====
C
C UNITS:
C Times Values of Type REAL are in seconds
C of Type INTEGER*2 are in milli-seconds
C
C all other quantities are in SI units
C-----
C
C Structure for Data Base
C-----
C STRUCTURE /STORE/
C
C INTEGER SHOT /0/ ! Primary Key : Shot Number
C
C UNION
C MAP
C INTEGER DISR_TYPE /0/ ! Type of disruption
C END MAP ! (see Definition for Disruptions)
C MAP
C INTEGER*2 DISR_T1 ! Secondary key
C INTEGER*2 DISR_T2 !
C END MAP
C END UNION
C
C INTEGER*2 DATE(9)
C BYTE N_DISR /0/ ! total # disruptions
C BYTE N_D_S /0/ ! number of disruptions stored
C BYTE D_TYPE(2) /2*0/ ! criteria of disr recognition
C BYTE N_CAS /0/ ! # cascades after terminal disr
C BYTE YAG /0/ ! YAG data status
C (see Definitions for YAG data)
C INTEGER STATUS /0/ ! Status of read channels
C (see Definitions for channel status)
C
C Discharge History
C-----
C INTEGER*2 T_JP_MAX /0 / ! Time of Max plasma current (ms)
C INTEGER*2 T_NE_MAX /0 / ! Time of Max Electron Density
C INTEGER*2 T_Q_MIN /0 / ! Time of MIN q
C INTEGER*2 T_L1 /0 / ! Time of Lambda+1 (max)
C INTEGER*2 T_UL_MIN /0 / ! Time of UL_MIN
C INTEGER*2 T_DJP_M /0 / ! Time of max djP/dt
C INTEGER*2 T_DNE_M /0 / ! Time of max dne/dt
C INTEGER*2 T_NE_BAD /0 / ! Time when ne becomes invalid
C INTEGER*2 TTOT /0 / ! Total discharge duration
C REAL T_TOP /0./ ! time start of plateau (sec)
C REAL T_TOP_E /0./ ! time end of plateau
C REAL T_END /0./ ! time end of discharge
C REAL BT /0./ ! Toroidal field
C REAL JP_MAX /0./ ! Max plasma current

```


REAL	NE_MAX	/0./	! Max Electron Density
REAL	NE_MAX_JP	/0./	! Plasma Current to NE_MAX
REAL	Q_MIN	/0./	! MIN q
REAL	LI(2)	/2*0./	! Lambda+1 (max + plateau)
REAL	UL_MIN	/0./	! min Uloop
REAL	UL	/0./	! Uloop in plateau
REAL	DJP_MAX	/0./	! max dJP/dt
REAL	DNE_MAX	/0./	! max dne/dt
REAL	E_TOT	/0./	! total energy (OH input)
REAL	E_ICRH	/0./	! ICRH Power input
REAL	E_LH	/0./	! LH Power input
REAL	E_NI	/0./	! NI Power input
REAL	PRAD	/0./	! Radiation (output)
REAL	ZEFF	/0./	! Zeff (Spitzer - Te)
REAL	ZEFF_2	/0./	! Zeff (Steuer)
REAL	LI	/0./	! li (Spitzer - Te)
REAL	TS_ICRH	/0./	! Start of ICRH
REAL	TE_ICRH	/0./	! End of ICRH
REAL	ICRH	/0./	! max ICRH
REAL	TS_LH	/0./	! Start of Lower Hybrid
REAL	TE_LH	/0./	! End of Lower Hybrid
REAL	LH	/0./	! max Lower Hybrid
REAL	TS_NI	/0./	! Start of Neutral Injection
REAL	TE_NI	/0./	! End of Neutral Injection
REAL	NI	/0./	! max Neutral Injection
REAL	TS_L	/0./	! Start of LOCK mode
REAL	TE_L	/0./	! End of LOCK mode

C

C Plasma Conditions at first and terminal disruption

C-----

REAL	T_DISR(2)	/2*0./	! time of disruption
REAL	JP_DISR(2)	/2*0./	! JP at disruption
REAL	NE_DISR(2)	/2*0./	! ne at disruption
REAL	L_DISR(2)	/2*0./	! Lambda+1 at disruption
REAL	Q_DISR(2)	/2*0./	! q at disruption
REAL	DJP_AV(2)	/2*0./	! dJP/dt everage for 50ms bef disr
REAL	DNE_AV(2)	/2*0./	! dne/dt everage for 50ms bef disr
REAL	ULOOP(2)	/2*0./	! Loop Voltage inside vessel
REAL	R(2)	/2*0./	! major radius of plasma
REAL	Z(2)	/2*0./	! vertical position of plasma
REAL	PRAD_D(2)	/2*0./	! Radiation
REAL	ZEFF_2 D(2)	/2*0./	! Zeff (Steuer) at disruption
REAL	ZEFF_DISR(2)	/2*0./	! Zeff (Spitzer - Te) at disruption
REAL	LI_DISR(2)	/2*0./	! li (Te) at disruption

C

C Plasma dynamics during disruption

C-----

REAL	MHD(2)	/2*0./	! MHD precursor characterization
REAL	FLUX(2)	/2*0./	! Total expelled flux
REAL	DJP_JP	/0./	! max dJP/dt / JP
REAL	DHOR	/0./	! horizontal displacement
REAL	DVER	/0./	! vertical displacement
REAL	X_RAY	/0./	! max count +- 3ms
REAL	X_PRE	/0./	! max count 100ms prior disr
REAL	TX_PRE	/0./	! Time of x_PRE
REAL	R_J_MAX	/0./	! max Rt-R20 * JP
REAL	Z_J_MAX	/0./	! max zt-z20 * JP

C

C General machine preconditions

C-----

INTEGER*2	N_OPEN	/0/	! shot since machine opening
INTEGER*2	N_DC	/0/	! shot since discharge cleaning
INTEGER*2	N_ARGON	/0/	! shot since argon
INTEGER*2	N_BOR	/0/	! shot since boron
INTEGER*2	N_CARBON	/0/	! shot since carbon
INTEGER*2	N_D2	/0/	! shot since D2

```

        INTEGER*2    N_HE      /0/      ! shot since helium
        INTEGER*2    N_TI      /0/      ! shot since titanium
        BYTE         N_DAY      /0/      ! shot of day
        BYTE         CARBON     /0/      ! carbonization
        BYTE         DIVERTOR   /0/      ! divertor configuration
C                                     (see Definitions for Divertor)
        BYTE         GETTER     /0/      ! gettering
        BYTE         HEAT       /0/      ! additional heating info
C                                     (see Definitions for Heat)
        BYTE         PELLET     /0/      ! Pellet Injection
        BYTE         PLASMA     /0/      ! Type of plasma
C                                     (see Definitions for Plasma)
        BYTE         MODE       /0/      ! Plasma Mode (HMODE.LIST)
C                                     ! (see Definitions for MODE)
        BYTE         SAW        /0/      ! Saw teeth
        INTEGER*2    MAC_T      /0/      ! Themes from MAC log
C                                     (UEBERSICHT.DAT)
        BYTE         MAC_G(3)   /3*0/    ! General Info from MAC log
C                                     (see Definitions for MAC)
        INTEGER*2    PHASE      /0/      ! LH Phase
        CHARACTER*14 COMMENT    /' '/    ! (available for future use)
END STRUCTURE

```

400 Bytes / 100 Words

```

C
C
C Definitions for channel status (availability of raw data)
C -----

```

C Bits to be set in S.STATUS

```

C
        INTEGER     CH_JP      ! Plasma current valid
        INTEGER     CH_JP30    ! if set 30,JPLAS; else 31,JPLAS1
        INTEGER     CH_MAG     ! 31,IUIDT,IUADT; magnetic data valid
        INTEGER     CH_ULOOP   ! 30 ULOOP
        INTEGER     CH_NE      ! valid density
        INTEGER     CH_NE2     ! if set 30,DICHTE; else 44,H1
        INTEGER     CH_NE_INV  ! NE becomes invalid during discharge
        INTEGER     CH_NE_INV2 ! NE not valid after disruption
        INTEGER     CH_Q       ! 31,BPHI
        INTEGER     CH_DISPL   ! 31,DHOR,DVER; displacement
        INTEGER     CH_MHD     ! 33,MHDA
        INTEGER     CH_X       ! 22,R1; X-Ray
        INTEGER     CH_PRAD    ! 180,PRAD1
        INTEGER     CH_GASV    ! 30,GASV
        INTEGER     CH_LH_MAC  ! Info from LH MAC files
C                                     (Soeldner)
        INTEGER     CH_LOCK    ! 30,LOCK
        INTEGER     CH_MYK     ! Info from MYKENN
C                                     (Mertens, Sandmann)
        INTEGER     CH_MAC     ! Info from MAC
C                                     (Niedermeier)
        INTEGER     CH_MODE    ! Info from HMODE.LIST
C                                     (Kus)
        INTEGER     CH_HEAT    ! Additional Heat
        INTEGER     CH_NI      ! 5,PNI; Neutral Injection
        INTEGER     CH_NI2     ! 31,NI; Neutral Injection
        INTEGER     CH_LH      ! 30,LH; Lower Hybrid
        INTEGER     CH_ICRH    ! 30,ICRH
        INTEGER     CH_PELLET  ! Pellet Injection
        INTEGER     TERM_DISR  ! terminal disruption

```

```

C
        PARAMETER (CH_JP30 =0)
        PARAMETER (CH_JP   =1)
        PARAMETER (CH_MAG   =2)
        PARAMETER (CH_ULOOP =3)
        PARAMETER (CH_NE    =4)
        PARAMETER (CH_NE2   =5)
        PARAMETER (CH_Q     =6)

```

```

PARAMETER (CH_DISPL =7)
PARAMETER (CH_MHD =8)
PARAMETER (CH_X =10)
PARAMETER (CH_PRAD =11)
PARAMETER (CH_GASV =12)
PARAMETER (CH_MYK =13)
PARAMETER (CH_MAC =14)
PARAMETER (CH_HEAT =15)
PARAMETER (CH_NI =16)
PARAMETER (CH_NI2 =17)
PARAMETER (CH_LH =18)
PARAMETER (CH_ICRH =19)
PARAMETER (CH_PELLET=20)
PARAMETER (CH_NE_INV=21)
PARAMETER (CH_NE_INV2=22)
PARAMETER (CH_MODE =23)
PARAMETER (CH_LOCK =24)
PARAMETER (CH_LH_MAC=25)
PARAMETER (TERM_DISR=31)

```

C
C Definitions for Disruption

C-----

C Bits to be set in S.DISR_TYPE

```

INTEGER      DSR_RISE      ! during current rise
INTEGER      DSR_PLAT     ! during current plateau
INTEGER      DSR_DECAY    ! during current decay
INTEGER      DSR_DNSTY    ! during density increase
INTEGER      DSR_HEAT     ! during additional heating
INTEGER      DSR_ICRH     ! during ICRH heating
INTEGER      DSR_LH       ! during Lower Hybrid
INTEGER      DSR_NI       ! during Neutral Injection

```

C

```

PARAMETER    (DSR_RISE = 4)
PARAMETER    (DSR_PLAT = 3)
PARAMETER    (DSR_DECAY = 2)
PARAMETER    (DSR_DNSTY = 1)
PARAMETER    (DSR_HEAT = 0)
PARAMETER    (DSR_ICRH = 16)
PARAMETER    (DSR_LH = 17)
PARAMETER    (DSR_NI = 18)

```

C

C Definitions for additional heating

C-----

C Bits to be set in S.HEAT

```

INTEGER      H_NI        ! neutral injection (any)
INTEGER      H_NICO     ! neutral injection co
INTEGER      H_NICN     ! neutral injection counter
INTEGER      H_ICRH     ! ion cyclotron resonance
INTEGER      H_LH       ! lower hybrid

```

C

```

PARAMETER    (H_NI = 0)
PARAMETER    (H_NICO = 1)
PARAMETER    (H_NICN = 2)
PARAMETER    (H_ICRH = 3)
PARAMETER    (H_LH = 4)

```

C

C Definitions for YAG Data

C-----

C Bits to be set in S.YAG

```

INTEGER      Y_PROC     ! YAG data processed
INTEGER      Y_VALID    ! valid YAG data exist
INTEGER      Y_TOP      ! valid YAG data for flat top
INTEGER      Y_DISR_1   ! valid YAG data for disruption
INTEGER      Y_DISR_2   ! valid YAG data for disruption

```

C

```

PARAMETER    (Y_PROC = 0)

```

```

PARAMETER      (Y_VALID = 1)
PARAMETER      (Y_TOP   = 2)
PARAMETER      (Y_DISR_1= 3)
PARAMETER      (Y_DISR_2= 4)
C
C Definitions for Divertor
C-----
C Bits to be set in S.DIVERTOR      ( to be set by MYK or MAC )
INTEGER        D_DN                  ! double null
INTEGER        D_SNU                  ! single null up
INTEGER        D_SND                  ! single null down
INTEGER        D_LIM                  ! limiter
C
PARAMETER      (D_DN   = 0)
PARAMETER      (D_SNU  = 1)
PARAMETER      (D_SND  = 2)
PARAMETER      (D_LIM  = 3)
C
C Definitions for Plasma
C-----
C Bits to be set in S.PLASMA and S.MODE (MYK / HMODE)
INTEGER        P_H                    ! Hydrogen
INTEGER        P_D                    ! Deuterium
INTEGER        P_HE                   ! Helium
C
PARAMETER      (P_H   = 0)
PARAMETER      (P_D   = 1)
PARAMETER      (P_HE  = 2)
C
C Definitions for Plasma MODE          (HMODE.LIST)
C-----
C Bits to be set in S.MODE
INTEGER        MODE_H                  ! H mode
INTEGER        MODE_BH                 ! Beam was Hydrogen
INTEGER        MODE_BD                 ! Beam was Deuterium
INTEGER        MODE_BHE                ! Beam was Helium
INTEGER        MODE_NI                 ! Max S.NI is from HMODE.LIST
C
PARAMETER      (MODE_H = 7)
PARAMETER      (MODE_NI = 6)
PARAMETER      (MODE_BD = 5)
PARAMETER      (MODE_BH = 4)
PARAMETER      (MODE_BHE = 3)
C
C Definitions for MAC                  (UEBERSICHT.DAT)
C-----
C
INTEGER        M_BLM                   ! Beta Limit
INTEGER        M_CNT                   ! Counter Injection
INTEGER        M_COND                  ! Machine Conditioning
INTEGER        M_CONF                  ! Confinement studies
INTEGER        M_DIAG                  ! Shots for a diagnostic
INTEGER        M_DIOP                  ! Divertor optimization
INTEGER        M_DIV                   ! Divertor physic
INTEGER        M_DLM                   ! Density Limit
INTEGER        M_DOKU                  ! Documentation
INTEGER        M_DTST                  ! Test of impurities
INTEGER        M_EICH                  ! Calibration
INTEGER        M_FIR                   ! Ferninfrared - Laser
INTEGER        M_FLUC                  ! Fluctuation studies
INTEGER        M_HBPO                  ! High Beta Poloidal Studies
INTEGER        M_HMOD                  ! H mode studies
INTEGER        M_ICON                  ! Impuls Confinement Studies
INTEGER        M_IMPU                  ! Impurity studies
INTEGER        M_INBE                  ! Start of something
INTEGER        M_IOC                   ! IOC

```

INTEGER	M_ISOT	! Isotope Effect
INTEGER	M_KSZ	! Shots without sawteeth (intent)
INTEGER	M_LMOD	! L mode studies
INTEGER	M_MHD	! MHD
INTEGER	M_MOD	! mode studies
INTEGER	M_MP	! Multipol
INTEGER	M_NEUT	! Neutron measures
INTEGER	M_OPTI	! Optimization general
INTEGER	M_PART	! Partical transport
INTEGER	M_PROF	! Profile studies
INTEGER	M_QLIM	! q-Limit
INTEGER	M_SPEC	! Spectroscopy studies
INTEGER	M_STD	! Standard discharge
INTEGER	M_SZ	! Saw Tooth Instability
INTEGER	M_TECH	! Technical shot
INTEGER	M_TEST	! Test shot

C

PARAMETER	(M_BLM	= 1)	! These are values NOT bits
PARAMETER	(M_COND	= 2)	
PARAMETER	(M_CONF	= 3)	
PARAMETER	(M_DIAG	= 4)	
PARAMETER	(M_DIOP	= 5)	
PARAMETER	(M_DIV	= 6)	
PARAMETER	(M_DLIM	= 7)	
PARAMETER	(M_DTST	= 8)	
PARAMETER	(M_EICH	= 9)	
PARAMETER	(M_FLUC	=10)	
PARAMETER	(M_HMOD	=11)	
PARAMETER	(M_IMPU	=12)	
PARAMETER	(M_INBE	=13)	
PARAMETER	(M_IOC	=14)	
PARAMETER	(M_MHD	=15)	
PARAMETER	(M_MP	=16)	
PARAMETER	(M_NEUT	=17)	
PARAMETER	(M_OPTI	=18)	
PARAMETER	(M_PART	=19)	
PARAMETER	(M_QLIM	=20)	
PARAMETER	(M_SPEC	=21)	
PARAMETER	(M_STD	=22)	
PARAMETER	(M_SZ	=23)	
PARAMETER	(M_TECH	=24)	
PARAMETER	(M_TEST	=25)	
PARAMETER	(M_CNT	=26)	
PARAMETER	(M_DOKU	=27)	
PARAMETER	(M_FIR	=28)	
PARAMETER	(M_HBPO	=29)	
PARAMETER	(M_ICON	=30)	
PARAMETER	(M_ISOT	=31)	
PARAMETER	(M_KSZ	=32)	
PARAMETER	(M_LMOD	=33)	
PARAMETER	(M_MOD	=34)	
PARAMETER	(M_PROF	=35)	